ELSEVIER

Physica C 317–318 (1999) 117–126

PHYSICA C

Superconducting rare earth transition metal borocarbides

S.-L. Drechsler [a,*], S.V. Shulga [b], K.-H. Müller [a], G. Fuchs [a], J. Freudenberger [a], G. Behr [a], H. Eschrig [a], L. Schultz [a], M.S. Golden [a], H. von Lips [a], J. Fink [a], V.N. Narozhnyi [a], H. Rosner [c], P. Zahn [c], A. Gladun [c], D. Lipp [c], A. Kreyssig [c], M. Loewenhaupt [c], K. Koepernik [c], K. Winzer [d], K. Krug [d]

[a] *Institut für Festkörper- und Werkstofforschung Dresden, D-01171 Dresden, Postfach 270016, Germany*
[b] *Institute of Spectroscopy, RAS, Troitsk, Russian Federation*
[c] *Technische Universität Dresden, Dresden, Germany*
[d] *1. Physikalisches Institut, Georg-August-Universität Göttingen, Göttingen, Germany*

Abstract

We present an overview of selected properties of quaternary intermetallic rare earth transition metal borocarbides and related boronitride compounds, as well as of theoretical calculations with possible relevance to the mechanism of superconductivity. The interplay of superconductivity and magnetism for compounds with pure and mixed rare earth components is considered. We suggest that the incommensurate magnetic structure modulated along the *a*-axis is responsible for the pair breaking in $Ho_xR_{1-x}Ni_2B_2C$; R = Y, Lu samples. The effect of doping (Cu, Co) at the transition metal site is considered experimentally and theoretically. The possible role of correlation effects due to the presence of the transition metal component in determining the electronic structure is discussed comparing the band structure calculation results with various electronic spectroscopies as well as de Haas–van Alphen data. Important thermodynamic properties of these systems are analyzed within multiband Eliashberg theory with special emphasis on the upper critical field $H_{c2}(T)$ and the specific heat. In particular, the unusual positive curvature of $H_{c2}(T)$ near T_c observed for high-quality single crystals, polycrystalline samples of YNi_2B_2C, $LuNi_2B_2C$ as well as to a somewhat reduced extent also for the mixed system $Y_{1-x}Lu_xNi_2B_2C$ is explained microscopically. It is shown that in these well-defined samples the clean limit of type II superconductors is achieved. The values of $H_{c2}(T)$ and of its positive curvature near T_c (as determined both resistively and from magnetization as well as from specific heat measurements is an intrinsic quantity generic for such samples) *decrease* with growing impurity content. Both quantities thus provide a direct measure of the sample quality.

Keywords: Metal borocarbides; Local density approximation (LDA); Superconductivity

1. Introduction

Five years after the discovery [1–4] of rare earth transition metal borocarbides (nitrides) (RTBC(N)) with T = Ni, Pd, Pt transition metals, the place of RTBC(N) compounds within the family of more or less exotic superconductors is still under debate. In contrast to first speculations of a strong similarity to quasi-2D cuprates (suggested by their reminiscent transition metal layered crystal structure), various LDA (local density approximation) band structure

* Corresponding author. Fax: +49-351-4659-537; E-mail: drechsler@ifw-dresden.de

0921-4534/99/$ - see front matter
PII: S0921-4534(99)00051-9

calculations performed in 1994/1995 (see Refs. [5–17]) clearly demonstrated their 3D electronic structure. Consequently, the whole class has been classified as traditional superconductors, more or less closely related to the A-15's or to other intermetallic compounds. Only the interplay of antiferromagnetism and superconductivity for R = Ho, Er, Dy, Tm, Tb, Pr has been regarded as a challenging problem of general interest. However, during the last two years the situation for non-magnetic borocarbides has been changed considerably as high-quality single crystals have become available revealing (i) more pronounced anisotropies for $LuNi_2B_2C$ [18] (some of them even being strongly temperature dependent) in contrast to the first experimental observations [19] for YNi_2B_2C and (ii) the clear multiband character of the superconducting state in YNi_2B_2C and $LuNi_2B_2C$ [20]. The value of the gap ratio $2\Delta/T_c$, initially fixed to the conventional BCS value 3.5, now varies from 0.45 [21] to 3.2 [22–24]. Finally, in the context of anisotropy and other unusual properties (see below), *d*-wave superconductivity has been proposed for YNi_2B_2C and $LuNi_2B_2C$ [25–27]. Quite interestingly, other RTBC(N) superconductors such as $(LaN)_3(NiB)_2$ show more standard *s*-wavelike behaviour [28]. Analyzing available structural data and band structure results, we propose a qualitative semi-microscopic scenario for this striking different behaviour.

2. Crystal structure and critical temperature

The tetragonal layered crystal structures of the $I4/mmm$ or $P4/nmm$ types resolved so far for all well characterized RTBC(N) compounds can be written schematically as $(RC(N))_n(TB)_2$ with $n = 1,2,3$. There are systematic dependences of T_c with increasing T–T distance, the transition metal component T = Ni, Pd, Pt and the dopants replacing the T: T′ = Cu, Co, V, etc., and/or the B–T–B bond angle. Finally, the number of *metallic* layers separating and doping the $(NiB)_2$ networks also has a profound effect on the actual T_c value. Thus, for the single RC-layer (T = Ni) compounds the highest $T_c \approx 14$–16.6 K values are obtained for R = Sc, Y, Lu, whereas for R = Th it is reduced to ~ 8 K and it vanishes for R = La. The double-layer Lu, Y-compounds exhibit very small transition temperatures of 2.9 K and 0.7 K [28], respectively, which however can be increased considerably replacing Ni by Cu [29]. In the case of the two-layer boronitride $(LaN)_2(NiB)_2$ so far no superconductivity has been detected whereas the corresponding triple-layer compound exhibits a relatively high $T_c \approx 12$ K. Details of what appear to be the cubic crystal structures of several metastable Pd-based compounds showing in some cases $T_c \geq 21$ K have not been resolved till now.

3. The electronic structure

All bandstructure calculations [5–17] reveal sizeable dispersion in *c*-direction of the bands crossing the Fermi level and fluctuation magnetoconductance measurements [30] clearly demonstrate the 3D nature of the superconductivity under consideration. Electronically the coupling of the 2D-$(TB)_2$ networks is mediated mainly by the carbon/nitrogen $2p_z$ states. Further, important issues are the peak of the density of states (DOS) $N(0)$ near the Fermi level $E_F = 0$ and the intermediate strength of correlation effects.

3.1. LDA calculations

The electronic structure near $E_F = 0$ of all RTBC(N) compounds is characterized by a special band complex containing three or four bands (total width about 3 eV, see Fig. 1 for the case of $LaPt_2B_2C$) above the main group of T-derived *d*-states (total width about 7 eV). For $Lu(Y)Ni_2B_2C$ there is a flat band near E_F giving rise to a narrow asymmetric peak in the total DOS $N(E)$ and to a large T-*d*-partial DOS $N_d(0) \approx 0.5\ N(0)$ which can be analyzed with high accuracy within our LCAO-method (linear combination of atomic-like orbitals) calculational scheme [31]. For most of the other RTBC-superconductors $N(0)$ and especially $N_d(0)$ are reduced. However, there is no simple relation between the calculated value of $N(0)$ and the measured T_c-value (see Fig. 2). Notice that our full

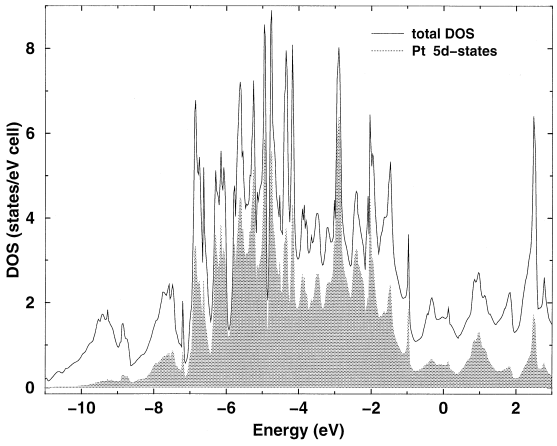

Fig. 1. LCAO–LDA full relativistic total DOS (solid line) and Pt-partial 5*d* DOS (shaded) of $LaPt_2B_2C$; with the Fermi level at $E_F = 0$.

relativistic calculation for $LaPt_2B_2C$ yields a significantly reduced DOS $N(0) = 1.66$ states/eV cell compared with 2.5 obtained by Singh [8] where only the core states were treated fully relativistically and the valence states scalar relativistically. For our $N(0)$ the previous discrepancy with the specific heat data for $LaPt_{1.5}Au_{0.5}B_2C$ [32] and $LaPt_{1.7}Au_{0.3}B_2C$ [33] for the Sommerfeld constant $\gamma \propto N(0)(1 + \lambda)$ is removed: instead of an unreasonably small electron–phonon (el–ph) coupling constant $\lambda \approx 0.1$, we arrive now at more realistic values $\lambda \approx 0.66$ to 0.94, respectively. Our calculations for $Lu(Co_xNi_{1-x})_2B_2C$ within the LCAO-coherent potential approximation [34] show a strong reduction of $N(0)$ by about 21% and 42% for $x = 0.1$ and $x = 0.5$, respectively. The decrease of the Ni + Co related partial *d*-DOS is even stronger. All in all, the comparison with the available specific heat data reveals that most RTBC(N)-compounds exhibit intermediately strong el–ph interaction $\lambda \sim 0.5$ to 1.2, except $LaPd_2B_2C$ exhibiting extremely weak el–ph coupling.

3.2. Electronic spectroscopy and de Haas–van Alphen effect

Polarization dependent X-ray absorption spectroscopy (XAS) for an YNi_2B_2C single crystal probing the unoccupied electronic structure via transitions from the B(C) 1*s* core level into unoccupied states having B(C) $2p_x/2p_z$ symmetry are in reasonable agreement with the predictions of the LDA bandstructure calculations for the orbital-resolved partial DOS shown in Fig. 3. The covalency of the short C–B bond seems to be somewhat overestimated by the LDA predicting a smaller out-of-plane anisotropy than is observed in the XAS data. The observed isotropic Ni-related spectra are presumably dominated by effects of the strong $2p$ core hole $3d$

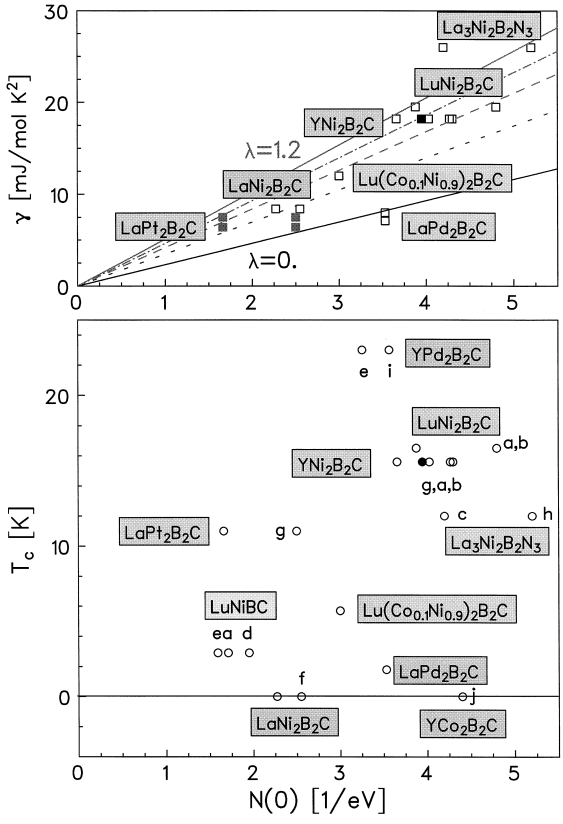

Fig. 2. Experimental values of the Sommerfeld constant (top) and the superconducting transition temperature T_c (bottom) vs. calculated total density of states at the Fermi level $N(0)$ (states per formula unit) for various RTBC(N)-compounds and different LDA-calculational schemes: Ref. [6]—(a), Ref. [5]—(b), Ref. [10]—(c), Ref. [15]—(d), Ref. [13]—(e), Ref. [8]—(g), Ref. [12]—(h), Ref. [9] (i), Ref. [7]—(f), Ref. [16]—(g), Ref. [12]—(h), Ref. [17]—(j). The straight lines in the upper picture denote various el–ph coupling constants $0 \le \lambda \le 1.2$ (dotted line: $\lambda = 0.5$, dashed line: $\lambda = 0.8$, dashed–dotted line: $\lambda = 1.0$).

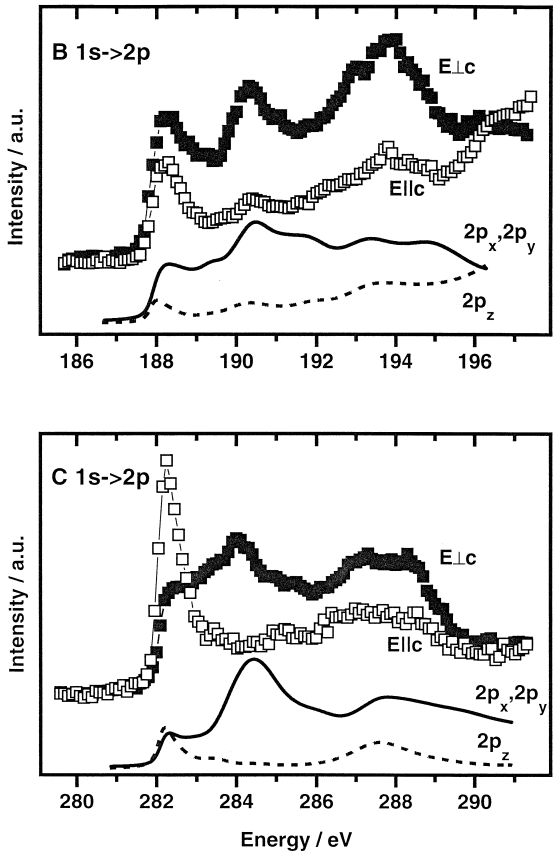

Fig. 3. Polarisation-dependent XAS spectra ($1s \rightarrow 2p$ transitions) of single crystal YNi_2B_2C are shown for boron (top) and carbon (bottom) with the electric field $\vec{E} \parallel$ and $\perp$ to the tetragonal c-axis (open and filled symbols, respectively). The corresponding m-resolved partial DOS from our LDA–LCAO calculations (see text) are denoted by dashed and full lines, and are broadened by account for life time and finite resolution effects.

Coulomb interaction. Therefore no direct comparison with the LDA prediction is possible. From a comparison of X-ray photoemission and Auger spectroscopy measurements a value of the Ni d–d Coulomb repulsion $U_d = 4.4 \pm 0.3$ eV [35] has been found which is intermediate between the values of 8 eV and 2 eV for strongly correlated NiO and weakly correlated Ni metal, respectively.

The most valuable insight into the electronic structure can be gained from de Haas–van Alphen (dHvA) measurements. In high-quality YNi_2B_2C single crystals up to six cross-sections are observed. The related Fermi velocities $v_{F,i}$, $i = 1,\ldots,6$, on extremal orbits can be grouped into two sets differing by a factor of 4. These observations and the sizable anisotropy of the H_{c2} for such crystals clearly indicate that they are nearly in the clean-limit regime. Further details of the Fermi surface can be obtained from the analysis of Hall data [36]. However, the observed qualitative differences between YNi_2B_2C and $LuNi_2B_2C$ as well as the large discrepancy between the experimentally and theoretically [5] predicted R_H-values are not well understood at present. To summarize, at the present status, there is a reasonable qualitative agreement between predictions of the LDA results and experimental data.

4. The upper critical field $H_{c2}(T)$

A detailed analysis of the magnitude and the shape of $H_{c2}(T)$ is given in Ref. [20]. In particular, the failure of the standard isotropic band approach points to a multiband description, where electrons with significantly smaller v_F compared with the Fermi surface average (see Fig. 4) $\sqrt{\langle v_F^2 \rangle_{FS}}$ and relatively strong el–ph coupling are mainly responsible for the superconductivity. This model explains also the strong deviations of the shape of $H_{c2}(T)$ from the standard parabolic-like curve and in particular also the positive curvature of $H_{c2}(T)$ near T_c. This curvature has very often been observed in resistivity measurements. In principle, it might be affected also by the flux state in fields $H \leq H_{c2}$. However, the fact that it has also been observed in magnetization and specific heat measurements (see Figs. 5 and 6) shows unambiguously that it is an inherent thermodynamic property generic for all clean RTBC(N) superconductors.

Fig. 4. Distribution of Fermi velocities v_F over the Fermi surface for $LuNi_2B_2C$ calculated from our LCAO band structure. The legend (bottom) gives the magnitude of v_F in atomic units. Γ points are at the corners of the volume shown. For clarity the Fermi surface has been divided into two separate diagrams.

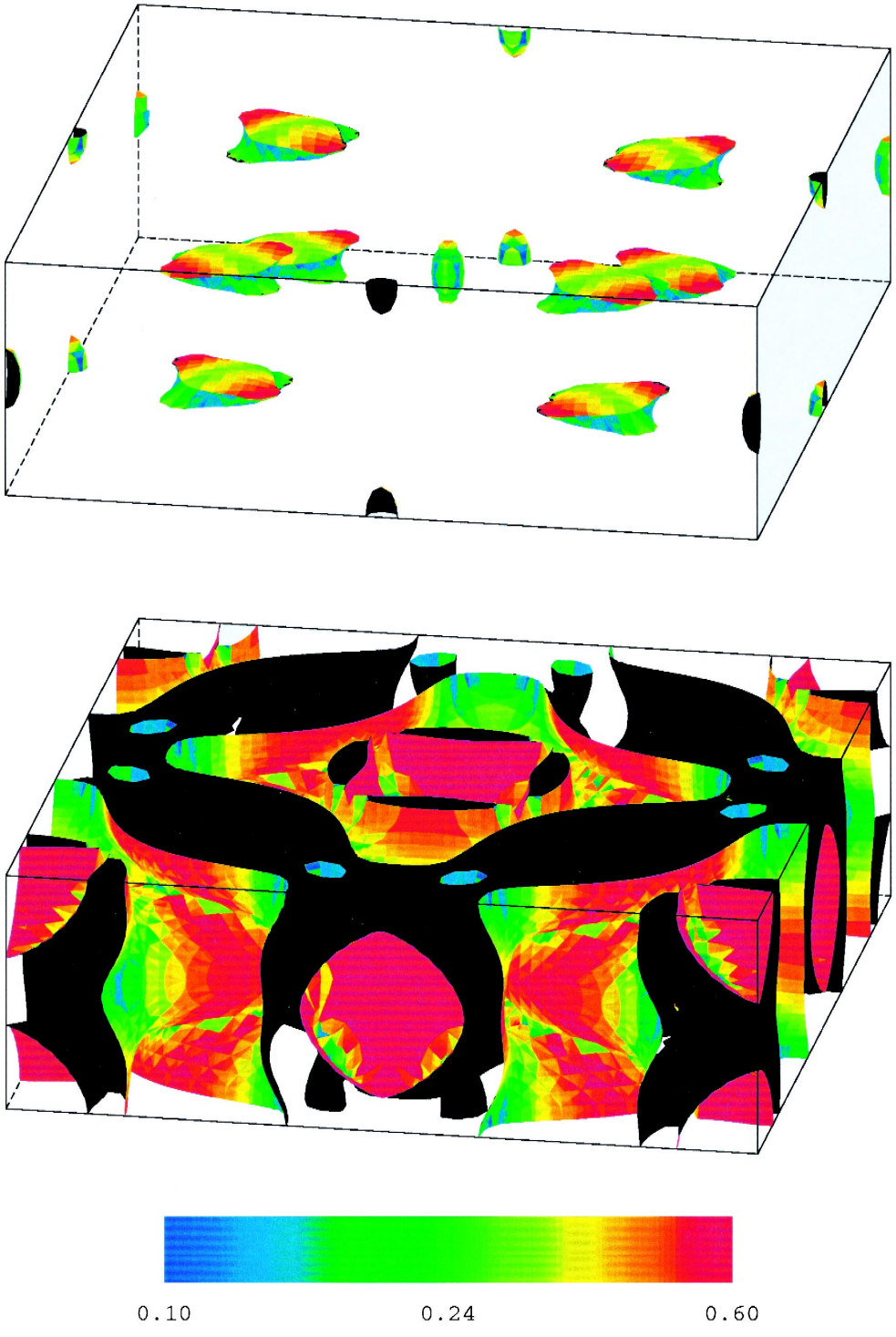
0.10
0.24
0.60

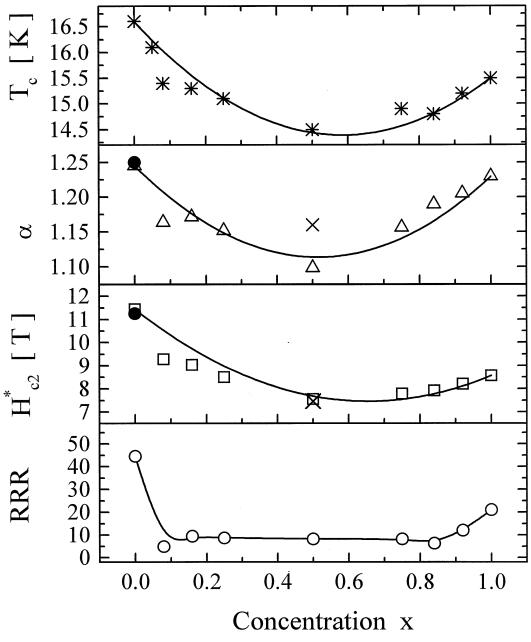

Fig. 5. The superconducting characteristics: T_c, the upper critical field parameters ($H^*_{c2}(0)$ and the curvature parameter α) determined from resistivity measurements and the resistivity ratio RRR for the mixed system $Y_xLu_{1-x}Ni_2B_2C$ vs. composition x. × (●) represents the results derived from the inset in Fig. 6, i.e., from the specific heat jump at $T_c(H)$, and from the magnetization (see Refs. [18,36]).

The inspection of the distribution of v_F over the Fermi surface of $LuNi_2B_2C$ derived from our LCAO–LDA calculations depicted in Fig. 4 yields that the major part of the electrons (dominating the normal state transport properties) exhibit large v_F-values (red and green) differing up to factor of 6 from the slow electrons (blue). This is in accord with our phenomenological analysis [20] of $H_{c2}(T)$ requiring a factor of 5 in their relative magnitudes. The electrons with low v_F's are found near those parts of the Fermi surface with nesting properties. Quite interestingly, vectors closely related to the nesting vector $q \approx 0.6\ 2\pi/a$, i.e., connecting the neighbouring blue parts (compare Fig. 3 of Ref. [15]), seem to occur also in low-frequency phonons exhibiting anomalously strong softening entering the superconducting state [37,38] as well as in the incommensurate a-xis modulated magnetic structure (see Fig. 7) which partially suppresses the superconductivity in low magnetic fields [39].

5. Disorder and doping

The reduction of the multiband effects discussed above can be studied by replacing partially some of the constituent atoms by entities with similar chemical and physical properties. Modest effects can be expected for chemically and magnetically equivalent substitutions R → R′ in the RC(N)-layer(s). For this purpose we have studied the crystal structure, T_c, $H_{c2}(T)$, and the specific heat of the mixed (polycrystalline) $Y_xLu_{1-x}Ni_2B_2C$ system [40]. Since the measured lattice constants a and c vary nearly linearly between the corresponding pure limits, a maximum of T_c might be expected for $x = 0.5$ according to the 'universal' curve $T_c = T_c(d_{Ni-Ni})$ proposed by Lai et al. [41], where d_{Ni-Ni} denotes the Ni–Ni distance. Instead of the expected maximum with $T_c \approx 17$ K we found a dip at $x = 0.5$ with $T_c \approx 14.5$ K as shown in Fig. 5. Also a reduction of the positive curvature which can be expressed conveniently over a wide temperature range by the exponent α

$$H_{c2}(T) \approx H^*_{c2}(0)(1 - T/T_c)^{\alpha},$$
$$0.3T_c \le T \le 0.95T_c. \qquad (1)$$

on going from high quality pure samples to mixed ones: $\alpha \approx 1.45$ (single crystals), 1.25 (polycrystalline samples) to $\alpha_\rho \approx 1.1$, $H^*_{c2,\rho}(0) = 7.6$ T derived from resistivity data and $\alpha_c = 1.16$, $H^*_{c2,C}(0) = 7.46$ T. from and specific heat data (see Figs. 5 and 6) is worth mentioning. Due to the saturation (negative curvature) at low T, $H^*_{c2}(0)$ can be regarded as an upper bound for the true $H_{c2}(0)$-value.

The residual resistivity ratio RRR = ρ(300 K)/$\rho(T_c)$ is strongly reduced by introducing only 8% 'big' Y impurities into the LuC layer: RRR = 48 → RRR = 8. The observed approximate plateau for $0.08 \le x \le 0.85$ might be interpreted in terms of strong scattering in the band (group of electrons) with large v_F, since $H_{c2}(T)$ is only slightly reduced. The relative jump of the electronic specific heat $\Delta C/\gamma T_c \approx 2.06$ at $x = 0.5$ is not very sensitive to impurity effects because it interpolates roughly between the limiting pure limits of 2.27(Lu) and 1.75(Y). The slight reduction of the Sommerfeld constant γ can be ascribed to a broadening of the peak in the DOS.

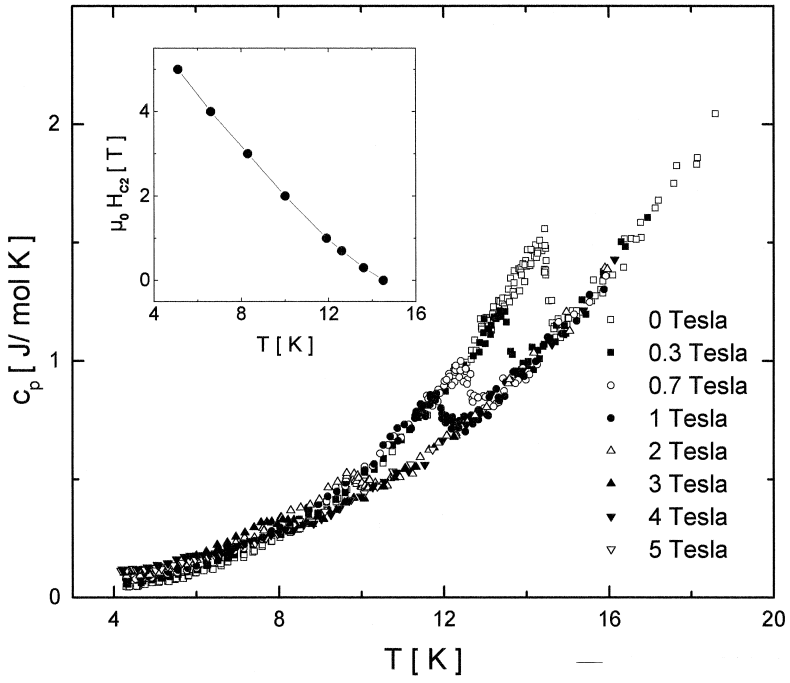

Fig. 6. The specific heat of $Y_{0.5}Lu_{0.5}Ni_2B_2C$ vs. temperature T. The inset shows the upper critical field determined from the jump at $T_c(H)$.

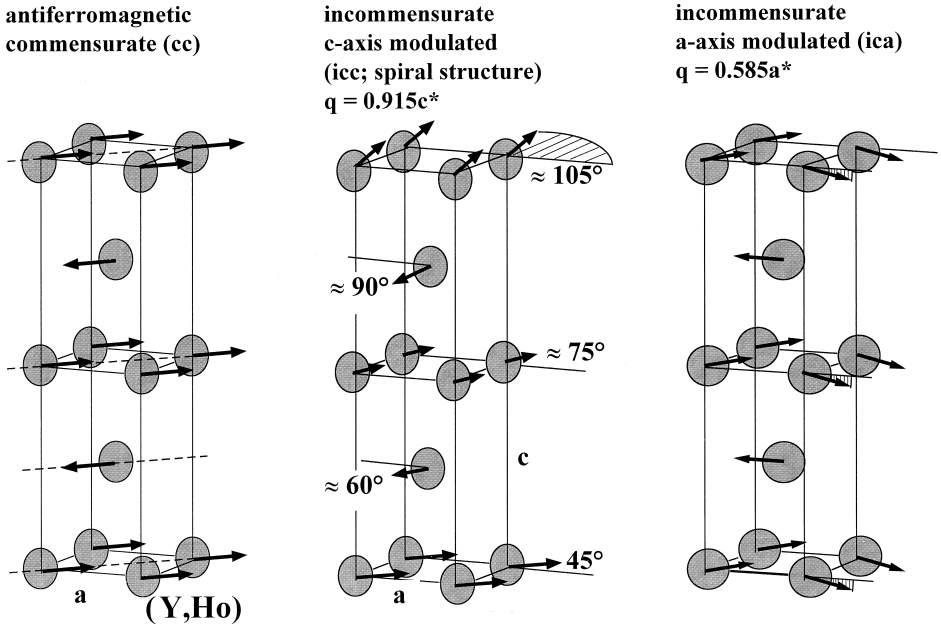

Fig. 7. Magnetic structures observed for the $HoNi_2B_2C$ compound.

6. Some aspects of magnetic borocarbides

The coexistence/competition of magnetism and superconductivity in borocarbides with magnetic rare earth elements is one of the most challenging problems in the field. Most dramatic effects have been observed for $HoNi_2B_2C$, where below the onset of superconductivity at 8.8 K a suppression of superconductivity (SSC) for $\vec{H} \perp$ to the *c*-axis and $4.5 \leq T \leq 5.5$ K has been detected as shown in Fig. 8. Three magnetic structures shown in Fig. 7 have been observed in this region: *c*-axis modulated commensurate (cc), the spiral *c*-axis modulated incommensurate (icc) and *a*-axis modulated incommensurate (ica) ones. From the fact the icc structure and the SSC both occur within a narrow temperature range and that these effects have only been observed for $HoNi_2B_2C$, it has been supposed that the icc structure is the origin for the SSC. However, replacing Ho partially by the nonmagnetic Y, the magnetic structures for $Y_xHo_{1-x}Ni_2B_2C$ are shifted *differently* to lower temperatures. This has enabled us [39] to identify the ica phase as the one responsible for the SSC-phenomenon. The observed vector in the *a*-modulated incommensurate structure $Q_m = 0.585\ a^*$ is close to the above mentioned calculated nesting vector of $0.6\ a^*$.

7. $LuNi_2B_2C$ and YNi_2B_2C: unconventional pairing?

For these two compounds there are several properties, which when taken together, might be interpreted as hints for unconventional (*d*-wave or *p*-wave) superconductivity, as follows.

(i) A $\sqrt{H}$-dependence of the electronic specific heat C_{el} in the superconducting state instead of the standard linear dependence.

(ii) The very weak damping of the dHvA oscilla-

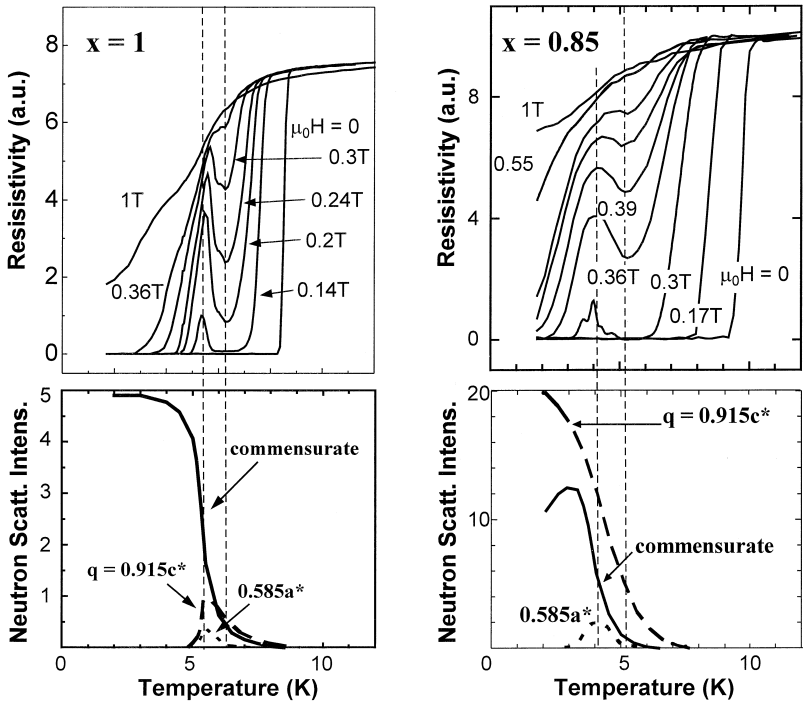

Fig. 8. Resistivity vs. temperature for various external magnetic fields for $Ho_xY_{1-x}Ni_2B_2C$ samples with $x = 1$ and $x = 0.85$ (top). Intensity of neutron scattering intensity vs. temperature for the magnetic structures explained in Fig. 7 (bottom).

tions in the superconducting state related to the superconducting gap has been interpreted as strong evidence for a very small or vanishing gap at parts of the Fermi surface [42].

(iii) A non-exponential *non-universal* power-like T-dependence of the electronic specific heat in the superconducting phase $C_{el} \propto T^{\beta}$, $\beta \sim 3$ at low temperatures ($\beta \approx 2.75$ for YNi_2B_2C [43] and $\beta > 3$ for $LuNi_2B_2C$ and $LaPt_2B_2C$). Strictly speaking, a pure one-band d-wave superconductor shows *quadratic* temperature dependence; a cubic dependence is expected for an order parameter with point-like nodes.

(iv) The anisotropy of $H_{c2}(T)$ within the basal plane of $LuNi_2B_2C$ [18] has been ascribed to d-wave pairing [25].

(v) A quadratic flux line lattice at high fields has been observed not only for magnetic RTBC but also for the non-magnetic title compounds [22–24],

(vi) Deviations from the Korringa behaviour of the nuclear spin lattice relaxation rate $1/T_1T = \text{const}$ have been ascribed to the presence of antiferromagnetic spin-fluctuations on the Ni site.

However, it should be noted that several of these unusual properties (i,iv,v) have been observed also for some more or less traditional superconductors such as V_3Si and $NbSe_2$. At present it is also unclear to what extent the observed anisotropies could be described alternatively by a full anisotropic (multiband) extended s-wave theory. Phase-sensitive experiments [44] and/or the observation of the Andreev bound state near appropriate surfaces[45] must be awaited to confirm or disprove the d-wave scenario.

Most importantly, some of the unusual T-dependences ascribed sometimes to the presence of antiferromagnetic spin fluctuations and 'non-Fermi liquid' effects might be caused by the rather strong energy dependence of the DOS near the Fermi level[16]. Finally, the observation of a weak Hebel–Slichter peak in the ^{13}C NMR data for the spin-lattice relaxation time T_1 $(1/T_1T)$ [46] must be mentioned. This points to the presence of at least one s-wave pairing component in the multiband order-parameter including also the C $2s$-electrons. However, a strong electron–electron interaction is suggested by the twice as large so-called enhancement factor $\alpha_c = 0.6$ compared with those of conventional 's-band' metals Li and Ag.

In this context, it should be mentioned that according to our LCAO calculations the C $2s$ contribution to $N(0)$ is very small ($\leq 1\%$).

8. A first attempt at a classification

Bearing the general similarities in the electronic and lattice structures of most RTB(N)-compounds in mind, we propose that essentially the same pairing mechanism should be responsible for all representatives. Since a substantial boron isotope effect has been measured for YNi_2B_2C and due to the absence of conclusive evidence for antiferromagnetic spin-fluctuations [16], the assumption of a dominating el–ph mechanism seems to be a quite natural one. In this case, the possible change of the order parameter symmetry (within a part of the multicomponent(band) order parameter) must be ascribed to the Coulomb repulsion. According to Varelogiannis [47], increasing for instance the Coulomb pseudopotential μ^*, one approaches a critical ratio μ^*/λ: below and above of which s-wave or d-wave superconductivity occurs, respectively. Due to the minimal extent of the $3d$ Wannier functions, the largest value of the on-site Coulomb interaction U can be expected in the case of the Ni-series. The presence of three intermediate LaN-layers in the triple-compound $(LaN)_3(NiB)_2$ might contribute to an additional screening of the onsite Coulomb interaction less pronounced in the single-layer compounds. Similarly, the presence of two Lu(Y)C-layers in Lu(Y)NiBC might be helpful to establish superconductivity at least at low temperatures absent in the single-layer compounds $LaNi_2B_2C$, YCo_2B_2C despite their larger $N(0)$-values (see Fig. 2). In general, the understanding of the absence of superconductivity in some of these compounds is of equal importance as the understanding of the representatives with the highest T_c-values. For the $4d$ and $5d$-members of the RTBC-family the DOS near the Fermi level $N(0)$ and especially the partial DOS with d-character $N_d(0)$ are reduced resulting possibly in a reduced Coulomb interaction, too.

9. Note added in proof

The investigation of two $Y_{1-x}Pt_xNi_2B_2C$, $x = 0$, 0.2 single crystals by Nohara et al. (cond-

mat/9902264, J. Phys. Soc. Jpn. 68 (4) (1999) in press) revealed for $x = 0.2$, despite the expected suppression of both $H_{c2}(T)$ and its positive curvature near T_c in approaching to the dirty limit, also the surprising complete suppression of the anomalous '*d*-wave like' negative curvature of the electronic specific heat $C_{el} \propto T\sqrt{H}$ in the mixed state. Since similar results have been obtained for the 'classical' extended *s*-wave superconductor $NbSe_2$ showing $C_{el} \propto T\,H^{0.66}$ in the low-T clean limit, (J.E. Sonier et al., cond-mat/9811420) in comparison with the standard behaviour $C_{el} \propto T\,H$ of the dirty counterpart system $Nb_{0.8}Ta_{0.2}Se_2$, the negative curvature of C_{el} has been considered as a general property of type-II superconductors in the clean limit, independent on the symmetry of the order parameter (A.P. Ramirez, Phys. Lett. A 211 (1996) 59). In particular, it might reflect the flux line core shrinkage due to vortex-vortex interactions (Ichioka et al., Phys. Rev. B 59 (1999) 184). Alternatively, the observation of Nahara et al. mentioned above might be interpreted as a consequence of the destruction of unconventional superconductivity present in the pure system because such a state is expected to be much more sensitive to disorder than the robust conventional *s*-wave one.

Acknowledgements

We would like to thank the Deutsche Forschungsgemeinschaft and the Sonderforschungsbereich 463 'Seltenerd-Übergangsmetallverbindungen: Struktur, Magnetismus und Transport' for financial support. Further support by the Graduiertenkolleg 'Struktur und Korrelationseffekte in Festkörpern' der TU Dresden is acknowledged (H.R.).

References

[1] C. Mazumdar et al., Solid State Commun. 87 (1993) 413.
[2] R. Nagarajan et al., Phys. Rev. Lett. 72 (1994) 274.
[3] R. Cava et al., Nature 376 (1994) 146.
[4] R. Cava et al., Nature 376 (1994) 252.
[5] W. Pickett, D. Singh, Phys. Rev. Lett. 72 (1994) 3702.
[6] L.F. Mattheiss, Phys. Rev. B 49 (13) (1994) 279.
[7] L.F. Mattheiss et al., Solid State Commun. 91 (1994) 587.
[8] D. Singh, Phys. Rev. B 50 (1994) 6486.
[9] W. Pickett, D. Singh, J. Supercond. 8 (1995) 425.
[10] D. Singh, W. Pickett, Phys. Rev. B 51 (1995) 8668.
[11] D. Singh, Solid State Commun. 98 (1995) 899.
[12] L.F. Mattheiss, Solid State Commun. 94 (1995) 741.
[13] R. Coehoorn, Physica C 228 (1994) 331.
[14] R.Y. Rhee et al., Phys. Rev. B 51 (15) (1995) 585.
[15] H. Kim et al., Phys. Rev. B 52 (1995) 4592.
[16] B.J. Suh et al., Phys. Rev. B 53 (1996) R6022.
[17] P. Ravindran et al., Phys. Rev. B 58 (1998) 3381.
[18] V. Metlushko et al., Phys. Rev. Lett. 79 (1997) 1738.
[19] M. Xu et al., Physica C 235 (1994) 2533.
[20] S.V. Shulga et al., Phys. Rev. Lett. 80 (1998) 1730.
[21] T. Jacobs et al., Phys. Rev. B 52 (1995) R7022.
[22] Y. de Wilde et al., Phys. Rev. Lett. 78 (1997) 4273.
[23] R. Eskildsen et al., Phys. Rev. Lett. 79 (1997) 487.
[24] M. Yethiraj et al., Phys. Rev. Lett. 78 (1997) 4849.
[25] G. Wang, K. Maki, Phys. Rev. B 58 (1998) 6493.
[26] M. Nohara et al., J. Phys. Soc. Jpn. 66 (1997) 1888.
[27] R. Takagi et al., Physica B 237–238 (1997) 292.
[28] G. Hilscher, H. Michor, in: A.V. Narlikar (Ed.), Studies of High Temperature Superconductors, Vols. 26–27, Nova Science Publishers, NY, 1998.
[29] A.K. Gangopadhyay, J.S. Schilling, Phys. Rev. B 54 (10) (1996) 107.
[30] M. Mun et al., Phys. Rev. B 56 (14) (1997) 668.
[31] H. Eschrig, Optimized LCAO Method, 1st edn., Springer-Verlag, Berlin, 1989.
[32] H. Michor et al., Phys. Rev. B 52 (16) (1995) 165.
[33] S.A. Carter et al., Phys. Rev. B 50 (1994) 4216.
[34] K. Koepernik et al., Phys. Rev. B 55 (1997) 5717.
[35] T. Böske et al., Solid State Commun. 98 (1996) 813.
[36] V.N. Narozhnyi et al., Solid State Commun. 109 (1999) 549, cond-mat/9902259.
[37] C. Stassis et al., these proceedings.
[38] M. Bullock et al., Phys. Rev. B 57 (1998) 7916.
[39] K.-H. Müller et al., J. Appl. Phys. 81 (1997) 4240.
[40] J. Freudenberger et al., Physica C 306 (1998) 1.
[41] C. Lai et al., Phys. Rev. B 51 (1995) 420.
[42] T. Terashima et al., Phys. Rev. B 56 (1997) 5120.
[43] N.M. Hong et al., Physica C 226 (1994) 85.
[44] D.A. Wollman et al., Phys. Rev. Lett. 71 (1993) 2134.
[45] C.-R. Hu, Phys. Rev. Lett. 72 (1994) 1526.
[46] T. Saito et al., J. Magn. Magn. Mater. 177–181 (1998) 557.
[47] G. Varelogiannis, Phys. Rev. B 57 (13) (1998) 743.